Distribution System Optimization Based on a Linear Power-Flow Formulation

Hamed Ahmadi, *Student Member, IEEE*, and José R. Martí, *Fellow, IEEE*

***Abstract*—In this paper, a framework for distribution system optimization is proposed. In this framework, different control variables, such as switchable capacitors, voltage regulators, and system configuration can be optimally determined to satisfy objectives, such as loss minimization and voltage profile improvement. Linearized power-flow equations are used in the optimization, and the problem is formulated as mixed-integer quadratic programming (MIQP), which has a guaranteed optimal solution. Existing efficient solution algorithms developed for MIQP problems facilitate the application of the proposed framework. System operational constraints, such as feeder ampacities, voltage drops, radiality, and the number of switching actions are considered in the model. The performance of the proposed framework is demonstrated using a variety of distribution test systems.**

***Index Terms*—Capacitor placement, distribution system optimization, mixed-integer quadratic programming (MIQP), reconfiguration, underload tap-changing transformers (ULTC) adjustment.**

I. Introduction

DISTRIBUTION systems (DS) are the "last mile" of a power system, delivering the power to the end users. Low-voltage (LV) levels, relatively large sizes, mixed cable, and overhead line sections, variable ranges of X/R, and radial (or weakly-meshed) configurations are amongst the well-known characteristics of DS. There are many control variables that affect the performance of DS, such as adjustment of underload tap-changing transformers (ULTC) and switchable capacitor banks, distributed generations, interruptible loads, and network configuration. Some widely used measures for evaluating the performance of DS are voltage profile [1], load balance among feeders and phases [2], network losses [2], service restoration time [3], as well as security and reliability [4]. Many studies have been conducted to find the optimum values for the control variables to achieve higher performance in DS. As mentioned before, there are many control variables and many objectives to optimize, and a variety of studies with different variables and objectives may be needed. The main focus of this paper, without loss of generality, is to minimize the losses in DS by optimally controlling capacitor banks, ULTCs, and network configuration.

It is more convenient to operate DS in radial configurations. Radiality, compared to other possibilities, leads to simpler control strategies, especially in protection. Nonetheless, there are normally open switches between feeders in different locations that can form loops between the feeders. Similarly, there are normally closed switches that can disconnect one section of a feeder. The first group is called tie switches (TS) and the second group is called sectionalizing switches (SS) [5]. By closing one TS and opening an appropriate SS, a new radial configuration can be achieved which may alter DS performance. This simple idea, called the *branch-exchange* algorithm, has previously been applied to find best configurations that provide minimum losses, for example, [2] and [6]–[9]. As a more detailed mathematical model, a binary variable can be designated to each line admittance which will then appear in nonlinear ac power-flow equations. This variable is zero if the line is open and one otherwise. These binary variables along with the nonlinear power-flow equations and objective function will form an optimization problem which belongs to the family of mixed-integer nonlinear programming (MINLP) problems. The MINLP problems are combinatorial problems which are well known for their complexity and computationally expensive features. Due to the lack of efficient mathematical approaches for solving this class of optimization problems within reasonable time, heuristic algorithms have been widely used in the literature to find fast, while suboptimal, solutions.

There are many heuristics that have been applied to the problem of DS reconfiguration with different characteristics. Genetic algorithms (GAs) have been utilized with improved characteristics in [10]–[14]. Other intelligent search algorithms have also been applied such as simulated annealing [15], ant colony [16], [17], harmony search algorithm [18], evolutionary algorithms [19]–[22], artificial neural networks (ANNs) [23], and particle swarm optimization [24]. Although some of these search algorithms have shown good performance, they might not be able to provide optimal solutions within the constraints of online applications. Besides, these methods may provide suboptimal solutions, and their optimality is usually not guaranteed.

Besides heuristic methods, there are also direct mathematical approaches available in the literature dealing with the DS reconfiguration problem. The Benders decomposition has been used in [25] to solve the MINLP problem by dividing it into two subproblems. Even though this approach has shown commendable

Manuscript received September 19, 2013; revised November 14, 2013; accepted January 14, 2014. Date of publication February 13, 2014; date of current version January 21, 2015. Paper no. TPWRD-01077-2013.

The authors are with the Department of Electrical and Computer Engineering, The University of British Columbia, Vancouver, BC V6T 1Z4 Canada (e-mail: hameda@ece.ubc.ca; jrms@ece.ubc.ca).

Digital Object Identifier 10.1109/TPWRD.2014.2300854

performance, the master problem is formulated as an MINLP, for which the existing commercial solvers have no guarantee to provide the optimum solution within a reasonable time.

The authors of [26] have proposed two reformulations of the reconfiguration problem, a mixed-integer conic programming (MICP) version and a mixed-integer linear programming (MILP) version. The computational efficiencies of the MICP and the MILP formulations have been compared. It is shown that in order to reach the optimal or near-optimal solution, the MICP is more time demanding than the MILP. However, in the case of large networks, the CPU time is relatively long for both of these methods. In addition, there are extra variables and constraints in the formulations that make the size of the problem unnecessarily large. It has to be noted though that this is an excellent study in the context of DS reconfiguration.

The authors of [27] have proposed another reformulation of reconfiguration problem which utilizes the *DistFlow* method (proposed by Baran *et al.*. in [2]) for power-flow calculations. The problem is converted into three different types of well-known optimization problems, namely, mixed-integer quadratic programming (MIQP), mixed-integer quadratically constrained programming, and second-order cone programming. The computation time for solving the first two problems has been shown to be relatively short; however, these formulations assume a fixed value for nodal voltages, which is not applicable if the system voltage profile has to be considered. The time required to solve the third formulation is drastically high and, therefore, not practical.

In this paper, a linear power-flow (LPF) formulation for DS is used instead of the conventional nonlinear equations. The LPF has been proposed by the present authors in [28]. In this method, loads are modeled considering their voltage dependence characteristics which allows for a load representation with a constant-impedance and a constant-current synthesis (Z-I model). Using this method, the DS optimization problems can be modeled as MIQP problems for which there is efficient commercial software available, such as CPLEX [29] and GUROBI [30]. The main advantages of the proposed framework are listed as follows.

- It is a general-purpose platform for DS optimization.
- It has a guaranteed optimal solution and the computation time is reasonable.
- The distance to the optimal solution (optimality gap) is known at each iteration, which provides an excellent stop criterion.
- No initial solution is required.
- The voltage dependency of the loads is taken into account which leads to more realistic results compared to the conventional constant power model for the loads.

The rest of this paper is organized as follows. In Section II, the load modeling and LPF formulation of [28] is reviewed. The proposed MIQP formulation for DS optimization is explained in Section III. In Section IV, the results obtained by applying the proposed method to a variety of test systems are demonstrated. The most important conclusions are summarized at the end of this paper.

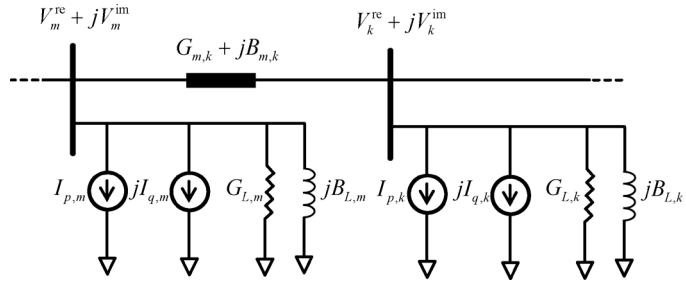

Fig. 1. Generic part of a DS derived based on the LPF formulation.

II. Linear Power-Flow Model

A. Load Modeling

A linear power-flow formulation for distribution systems was developed by the authors in [28]. The loads are modeled using two parallel components: 1) constant impedance and 2) constant current. This load model is obtained by fitting the load's voltage dependency with the following functions:

$$\frac{P(V)}{P_0} = C_Z \left(\frac{V}{V_0}\right)^2 + C_I \left(\frac{V}{V_0}\right) \tag{1}$$

$$\frac{Q(V)}{Q_0} = C'_Z \left(\frac{V}{V_0}\right)^2 + C'_I \left(\frac{V}{V_0}\right) \tag{2}$$

where P and Q are the load active and reactive power consumption, respectively; V is the terminal voltage magnitude; and the zero subscript stands for nominal values. Assuming that the measurement data are available for each load point, a curve-fitting algorithm based on least squares can be used to obtain the coefficients in (1) and (2), subject to the conditions $C_Z + C_I = 1$ and $C'_Z + C'_I = 1$. Without loss of generality, these coefficients are considered to be all equal to 0.5 in this paper. Typical values for load voltage dependencies can be found, for instance, in [31].

B. Linear Power-Flow Formulation

The Z-I load model described in Section II-A, together with the assumption of small voltage angles in DS, leads to the equivalent circuit shown in Fig. 1. The values for the equivalent admittance (G_L and B_L) and equivalent current source (I_p and I_q) for each load are obtained as

$$G_L = \frac{P_0 C_Z}{V_0^2}, \quad B_L = -\frac{Q_0 C'_Z}{V_0^2} \tag{3a}$$

$$I_p = \frac{P_0 C_I}{V_0}, \quad I_q = -\frac{Q_0 C'_I}{V_0}. \tag{3b}$$

Assuming the system admittance matrix as $\bar{Y} = \bar{G} + j\bar{B}$ and based on nodal analysis, the power-flow equations at node m can now be written as

$$\sum_{k=1}^{n} \left(\bar{G}_{m,k} V_k^{\mathrm{re}} - \bar{B}_{m,k} V\mathrm{im}_k\right) = I_{p,m} \tag{4}$$

$$\sum_{k=1}^{n} \left(\bar{G}_{m,k} V_k^{\mathrm{im}} + \bar{B}_{m,k} V\mathrm{re}_k\right) = I_{q,m} \tag{5}$$

where n is the number of nodes; m and k are the nodes at the two ends of the line connecting node m to node k; and V^{re} and V^{im} are the real and imaginary parts of the nodal voltages.

III. MIQP Formulations of Distribution System Optimization Problems

In this section, a platform for optimizing the operation of DS is developed. The three main control variables which contribute to the operation performance of DS are switchable capacitors, voltage regulators, and the configuration of the network. These variables are optimally controllable (with different objectives, such as loss reduction, load balancing, or voltage profile improvement) under the platform introduced in the following text.

A. Configuration

The most important part of the network reconfiguration formulation is how to model the status of the lines, that is, "on"/"off". The first method is to multiply the binary variables by the line flow limits, as done in [27]. The second method is to multiply the binary variables by the admittances of lines, which subsequently affects the admittance matrix. In the first method, if a line is offline, then its flow is forced to zero while in the second method, its impedance is forced to zero. The second method is followed here since the first method is not applicable in a nodal analysis formulation. The following equation describes the modified admittance of a line:

$$Y_{m,k} = \begin{cases} u_{m,k} y_{m,k} & m \neq k \\ -\sum\limits_{\substack{k=1 \\ k \neq m}}^{n} u_{m,k} y_{m,k} + jQ_{C,m} - Y_{L,m} & m = k \end{cases} \quad (6)$$

where Y $(= G + jB)$ is the modified admittance matrix; $y_{m,k}$ is the line admittance connecting node m to node k; Q_C and Y_L are the shunt capacitance and load admittance at each node, respectively; and $u_{m,k}$ stands for the line m-k status. Note that if there is no line between nodes m and k, the corresponding $u_{m,k}$ is zero.

The current flowing through line m-k ($I_{m,k}$) is calculated as

$$I_{m,k}^2 = u_{m,k}[G_{m,k}^2 + B_{m,k}^2][(V_m^{\mathrm{re}} - V_k^{\mathrm{re}})^2 + (V_m^{\mathrm{im}} - V_k^{\mathrm{im}})^2]. \quad (7)$$

The total network losses are given by the following formulas:

$$P_{\mathrm{loss}} = \sum_{\substack{m,k \\ m<k}} u_{m,k} G_{m,k} \left[(V_m^{\mathrm{re}} - V_k^{\mathrm{re}})^2 + (V\mathrm{im}_m - V_k^{\mathrm{im}})^2\right] \quad (8)$$

$$Q_{\mathrm{loss}} = -\sum_{\substack{m,k \\ m<k}} u_{m,k} B_{m,k} \left[(V_m^{\mathrm{re}} - V_k^{\mathrm{re}})^2 + (V_m^{\mathrm{im}} - V_k^{\mathrm{im}})^2\right]. \quad (9)$$

The condition of $m < k$ in (8) and (9) over the summations is necessary to avoid adding the losses of one line twice. Note that $u_{m,k} = u_{k,m}$.

To impose the radiality constraint, the formulation used in [26] is employed

$$\beta_{m,k} + \beta_{k,m} = u_{m,k} \quad (10a)$$

$$\sum_{k \in N_m} \beta_{m,k} = 1, \quad m \geq 2 \quad (10b)$$

$$\beta_{1,k} = 0, \quad k \in N_1 \quad (10c)$$

$$\beta_{m,k} \in \{0, 1\} \quad (10d)$$

where $\beta_{m,k}$ is 1 if node k is the parent of node m, and vice-versa; and N_m is the set of nodes directly connected to node m. Note that in [26], an extra continuous variable is defined to model line status. However, this extra variable ($u_{m,k}$) can be replaced by its definition in (10a). The structure of (10a) reveals that, at most, $\beta_{m,k}$ or $\beta_{k,m}$ should be 1. In the implementation, this characteristic can be translated into a special-ordered set (SOS) [32]. Most of the commercial software is able to take advantage of the SOS feature during the branch-and-bound (B&B) algorithm, which increases the speed of the solution procedure.

By substituting the equivalents of G and B in (4) and (5) from (6), bilinear terms will appear which are the results of multiplication of the line status (u) and nodal voltages (V^{re} and V^{im}). The problem of having the production of a binary variable (b) and a bounded continuous variable (x) can be solved by introducing a new continuous variable (z) and the following four inequality constraints [33]:

$$x - (1-b)x_{\max} \leq z \leq x - (1-b)x_{\min} \quad (11a)$$

$$bx_{\min} \leq z \leq bx_{\max}. \quad (11b)$$

If $b = 1$, then (11a) forces z to be equal to x and (11b) forces x $(= z)$ to lay within its bounds. If $b = 0$, then (11b) forces z to be zero and (11a) is the bounds on x. Therefore, z is equivalent to b times x. This technique is adopted here to eliminate the multiplication of binary continuous variables in (4) and (5). The new power-flow equations considering the status of the lines can be expressed by substituting (6) in (4) and (5) as follows:

$$\begin{aligned} &\sum_{\substack{k=1 \\ k \neq m}}^{n} \left[G_{m,k} V_k^{\mathrm{re}} u_{m,k} - B_{m,k} V_k^{\mathrm{im}} u_{m,k}\right] \\ &\quad - V_m^{\mathrm{re}} \left(\sum_{\substack{k=1 \\ k \neq m}}^{n} [G_{m,k} u_{m,k}] + G_{L,m} \right) \\ &\quad + V_m^{\mathrm{im}} \left(\sum_{\substack{k=1 \\ k \neq m}}^{n} [B_{m,k} u_{m,k}] + B_{L,m} + Q_{C,m} \right) = I_{p,m} \end{aligned} \quad (12)$$

$$\sum_{\substack{k=1 \\ k \neq m}}^{n} \left[G_{m,k} V_k^{\mathrm{im}} u_{m,k} + B_{m,k} V_k^{\mathrm{re}} u_{m,k}\right]$$

$$- V_m^{\mathrm{im}} \left(\sum_{\substack{k=1 \\ k \neq m}}^{n} [G_{m,k} u_{m,k}] + G_{L,m} \right) - V_m^{\mathrm{re}} \left(\sum_{\substack{k=1 \\ k \neq m}}^{n} [B_{m,k} u_{m,k}] + B_{L,m} + Q_{C,m} \right) = I_{q,m}. \tag{13}$$

Consider the nonlinear terms in (12) and (13) that are of the form $V_k^{\mathrm{re}} u_{m,k}$ and $V_k^{\mathrm{im}} u_{m,k}$. The following new variables are assigned to the binary continuous multiplications:

$$V_k^{\mathrm{re}} u_{m,k} \longrightarrow \alpha_{m,k}, \;\; V_k^{\mathrm{im}} u_{m,k} \longrightarrow \beta_{m,k} \;\; \forall m \in N_k. \tag{14}$$

Note that for each new variable, four inequality constraints should be added, as described in (11a) and (11b). All of the equations containing the bilinear terms should be updated according to the new variable definitions in (14). For instance, (7) can be reformulated as

$$I_{m,k}^2 = \left[G_{m,k}^2 + B_{m,k}^2\right] \left[\left(\alpha_{m,k} - \alpha_{k,m}\right)^2 + \left(\beta_{m,k} - \beta_{k,m}\right)^2 \right]. \tag{15}$$

The losses in (8) can be rewritten similar to (15). The power-flow equations in (12) and (13) are also updated by the new variables, that is, $\alpha_{m,k}$ and $\beta_{m,k}$.

There are security constraints imposed on the network reconfiguration process, such as feeder ampacities and the nodal voltage limits. These constraints are given as

$$I_{m,k}^2 \leq |I_{m,k}^{\max}|^2 \tag{16}$$

$$V_m^{\min} \leq \sqrt{V_m^{\mathrm{re}\,2} + V_m^{\mathrm{im}\,2}} \leq V_m^{\max}. \tag{17}$$

Recall the assumption of small voltage angles in DS made in [28]. That assumption also allows the elimination of the term $V_m^{\mathrm{im}\,2}$ in (17), giving the following box constraint:

$$V_m^{\min} \leq V_m^{\mathrm{re}} \leq V_m^{\max}. \tag{18}$$

Eventually, the DS reconfiguration problem for loss reduction will have (8) as its objective, subject to (10a)–(10d), (12)-(13), (15), (16), (18), and four sets of inequality constraints corresponding to each new variable $\alpha_{m,k}$ and $\beta_{m,k}$, as in (14). For instance, for $\alpha_{m,k} = V_k^{\mathrm{re}} u_{m,k}$, the additional constraints are

$$V_k^{\mathrm{re}} - (1 - u_{m,k}) V_{\max}^{\mathrm{re}} \leq \alpha_{m,k} \leq V_k^{\mathrm{re}} - (1 - u_{m,k}) V_{\min}^{\mathrm{re}} \tag{19a}$$

$$V_{\min}^{\mathrm{re}} u_{m,k} \leq \alpha_{m,k} \leq V^{\mathrm{re}} \mathrm{max} u_{m,k}. \tag{19b}$$

Good bounds for the real and imaginary parts of the voltages are chosen based on the system under study. Typical values are $V_{\min}^{\mathrm{re}} = 0.9$, $V_{\max}^{\mathrm{re}} = 1$, $V_{\min}^{\mathrm{im}} = -0.1$, and $V_{\max}^{\mathrm{im}} = 0.1$. It should be mentioned that the solution is not sensitive to these parameters and using the typical values suffices.

1) Limiting the Number of Switching Actions: As discussed before, in order to close a tie-switch (TS), it is inevitable that a sectionalizing switch (SS) must be opened to maintain radiality. The number of opening/closing actions, referred to as *switching actions*, should be limited due to the decrease in switches' lifetime. Moreover, numerous switching actions do not always lead to a significant reduction in losses, as shown in the next section. One way to limit the number of switching actions is to compare the current status of the switches to their initial status (u^0). Therefore, the total number of switching actions (S) can be calculated as

$$S = \sum_{\substack{m,k \\ m<k}} \left| u_{m,k} - u_{m,k}^0 \right|. \tag{20}$$

Every single element of the summation above can be either 0 or 1. This allows for replacing the absolute value operator ($|.|$) by a square operator

$$S = \sum_{\substack{m,k \\ m<k}} \left(u_{m,k} - u_{m,k}^0 \right)^2 = \sum_{\substack{m,k \\ m<k}} \left(u_{m,k} + u_{m,k}^0 - 2 u_{m,k} u_{m,k}^0 \right). \tag{21}$$

The recent equation is derived based on the fact that for a binary variable u, it follows that $u^2 = u$. Subsequently, (20) is linearized, as given in (21). The following constraint limits the maximum number of switching actions:

$$S \leq S^{\max} \tag{22}$$

where $S^{\max}$ is the maximum number of switching actions.

All of the equations forming the DS reconfiguration problem are linear except for (15) and (16), which are quadratic. Accordingly, the problem belongs to the family of MIQP problems.

B. Switchable Capacitors

In some systems, there are controllable capacitors along the feeders to compensate for the reactive power consumption and improve the voltage profile. Most of these capacitors have only one stage, while others may have more stages. Due to the variation of the demand, the number of online capacitors may need to change from time to time to adjust the system voltage profile and reduce the losses.

The online stages of a capacitor bank can be represented by an integer variable, for example, h, which indicates how many units are online. In the admittance matrix in (6), $Q_{C,m}$ represents the per-unit rating of the capacitor bank connected to node m. Multiplying the rating of each stage of the capacitor bank by an integer variable h_m allows for a mathematical formulation of the optimal control of capacitor banks. The power-flow equations are modified in a similar way as for the network reconfiguration problem in (12) and (13). The required equations can be derived by removing all $u_{m,k}$ and replacing $Q_{C,m}$ by $h_m Q_{C,m}$ in (12) and (13). The generated terms (product of voltages and

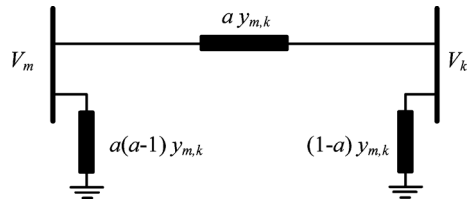

Fig. 2. Static model of the ULTC located between nodes m and k [34].

h_m) can be avoided the same way as described earlier in Section III-A. A limit is required for each capacitor bank indicating the number of stages available, as follows:

$$h_m \leq N_{C,m}^{\max} \tag{23}$$

where $N_{C,m}^{\max}$ is the maximum number of stages available for the capacitor bank connected at node m.

The problem of optimally controlling switchable capacitor banks will have (8) as its objective (by removing $u_{m,k}$) and modified version of (7), (12), (13), (16), (18), and (23) as its constraints. The result is an MIQP problem.

C. ULTC and Voltage Regulators

The transformers in a substation (or voltage regulators throughout the network) are usually equipped with ULTC capability to regulate the voltage according to the load variation. Besides improving the voltage profile, ULTC adjustment may also lead to loss reduction. Tap positions are discrete variables. In order to represent the ULTC capability in the proposed framework, the static model of ULTC described in [34] is used. This model is shown in Fig. 2, where a stands for the transformer ratio.

The design of the transformers is in such a way that the tap ratio usually varies between 0.9 to 1.1 ($\pm 10\%$). This fact allows for linearizing the term $a(a-1)$ in Fig. 2. A simple curve-fitting suggests that $a-1$ is approximately equivalent to $a(a-1)$ as long as a is close to 1. Obviously, the only parameters of the network that are affected by adding the ULTC adjustment variable (a) are the admittance matrix elements, that is, $\bar{G}$ and $\bar{B}$ in (4) and (5). The problem of having the multiplication of a and voltages can be solved by replacing the transformer ratio a by its discretized equivalent that covers all possible tap levels, for example, T levels, which are distributed evenly by a fixed difference, say T_p. Mathematically, a can be represented as

$$a = T_p^{\min} + T_p \sum_{i=1}^{T} w_i \tag{24}$$

where w_i is a binary variable. For example, if $T_p^{\min} = 0.9$ and $T_p = 0.05$, a tap position of $a = 1.05$ will be achieved by having only three of the binary variables equal to 1. The multiplications of binary continuous variables are linearized by the method described in (11a) and (11b).

Finally, the problem of ULTC adjustment for loss reduction has (8) as its objective, with all $u_{m,k}$ set to their initial values. The constraints are (4), (5), (7), (16), (18), (24), and four sets of inequality constraints corresponding to each auxiliary variable in (14) replacing the multiplications of binary continuous variables, that is, w_i multiplied by V_k^{re} and V_k^{im}.

TABLE I
DIMENSIONS OF THE TEST SYSTEMS

Test Case	Branches	Feeders	Load(MVA)
14-node	16	3	28.70 + i17.30
33-node	37	1	3.7 + i2.3
70-node	79	4	4.47 + i3.06
84-node	96	11	28.3 + i20.7
119-node	132	3	22.7 + i17.0
136-node	156	8	18.31 + i7.93
880-node	900	7	124.9 + i74.4

IV. NUMERICAL RESULTS

The performance of the proposed framework is evaluated using 6 test systems. The loads are modeled as voltage-dependent by (1) and (2). Six widely-used test systems, that is, the 14-node [6], 33-node [2], 70-node [35], 84-node [19], 119-node [36], 136-node [37], and 880-node [38] systems are obtained from corresponding references in which the system data is provided. Table I lists the characteristics of these test systems. The problems are formulated using the AIMMS language [39] and solved using the GUROBI [30] solver on an Intel Core i7-2600 CPU at 3.4 GHz and 8 GB of RAM computer. The *strong branching* method is used in the B&B algorithm. For node selection, *best bound* is chosen and seven parallel threads are used to solve the problems. In the following subsections, the results of different optimization problems are reported for the test systems.

A. Optimal Reconfiguration

The initial configuration of the test systems is given in the references from which the system data are obtained (see the previous paragraph). For the 14-node system, the capacitors are eliminated in this study. The initial tie switches are reproduced here in Table II. The initial losses, considering a constant-power load model, are also given in Table II. Table III shows the obtained results for DS reconfiguration for loss reduction for all of the test systems. The new tie switches are reported in Table IV. The power-flow solutions are obtained based on the voltage-dependent load model in (1) and (2) assuming $C_Z = C'_Z = 0.5$ for all loads. Note that other references use the constant-power model. The way loads are modeled here, which better reflects reality, has an intermediate effect on the total network losses. This can be explained by the fact that load values are given at a voltage of one per unit. However, when the voltages deviate from one per unit, the voltage-dependent loads consume a different amount of power, according to their voltage dependency characteristics.

It is worthwhile to briefly review the methods used in other references provided in Table III. In [19], network reconfiguration is formulated as a mixed-integer programming problem and is solved using mixed-integer hybrid differential evolution method. A mixed-integer convex programming formulation of the reconfiguration problem is proposed in [26] and is solved by

TABLE II
INITIAL CONFIGURATIONS AND LOSSES FOR TEST SYSTEMS

System	Losses (kW)	Open Lines
14-node	657.7	3-9,8-12,5-14
33-node	202.7	8-21,9-15,12-22,18-33,25-29
70-node	227.5	22-67,15-67,21-27,9-50,29-64,9-38,45-60, 38-43,9-15,39-59,15-46
84-node	532.0	5-55,7-60,11-43,12-72,13-76,14-18,16-26, 20-83,28-32,29-39,34-46,40-42,53-64
119-node	1298.1	27-48,17-27,8-24,45-56,51-65,38-65,9-42, 61-100,76-95,78-91,80-103,86-113,89-110, 115-123,25-36
136-node	320.4	7-86,10-32,20-130,46-223,33-61,59-145, 65-147,73-206,78-125,125-219,131-223, 139-154,138-217,138-153,141-154,141-220 ,145-206,160-56,212-122,215-123,223-147
880-node	3450.2	54-200,95-145,90-602,89-821,98-878,150-465,195-340,180-337,195-350,325-400, 330-450,345-500,455-600,458-800,463-824,460-440,580-800,585-824,500-870, 602-877,818-879,820-875,850-250,700-349,878-722,349-830,10-470

TABLE III
SIMULATION RESULTS FOR SYSTEM RECONFIGURATION: OPTIMAL SOLUTIONS

Test system	Source	P_{loss} (kW)	Q_{loss} (kVAR)	V_{min} (P.U.)	V_{avg} (P.U.)	CPU Time (s)
14-node	Initial*	593.9	683.9	0.955	0.979	-
	[19]	606.6	706.8	0.956	0.981	7.7
	MIQP*	553.7	645.7	0.959	0.981	0.14
33-node	Initial*	166.2	110.4	0.922	0.953	-
	[27]	140.0	104.9	0.941	0.967	12.8
	[40]	140.0	104.9	0.941	0.967	19
	MIQP*	122.8	90.0	0.943	0.968	3.2
70-node	Initial*	189.2	170.5	0.916	0.955	-
	[27]	205.3	192.5	0.927	0.952	11310
	MIQP*	172.3	158.6	0.937	0.957	5.7
84-node	Initial*	470.2	1213.6	0.936	0.972	-
	[19]	469.9	1251.4	0.953	0.972	36.2
	[26]	469.9	1251.4	0.953	0.972	207.7
	[40]	469.9	1251.4	0.953	0.972	3030
	MIQP*	424.2	1124.5	0.956	0.974	9.4
119-node	Initial*	1029.8	786.6	0.889	0.960	-
	[40]	853.6	726.9	0.917	0.966	4007
	MIQP*	765.9	553.7	0.938	0.969	39.4
136-node	Initial*	287.4	630.4	0.938	0.976	-
	[26]	280.2	611.3	0.959	0.977	>1800
	[40]	280.2	611.3	0.959	0.977	4473
	MIQP*	258.3	566.2	0.964	0.979	188.4
880-node**	Initial*	2858.8	2690.2	0.913	0.974	-
	[27]	999.1	1223.9	0.982	0.990	3192
	MIQP*	958.7	1172.0	0.982	0.990	1134

* In the MIQP and initial case, all loads are modeled as voltage-dependent with $C_Z = C'_Z = 0.5$. In other references, the loads are modeled as constant-power.
** Relative optimality gap is considered 1% for this case.

CPLEX. Different versions of mixed-integer programming formulation of the reconfiguration problem is given in [27] based on simplified assumptions. It should be noted that the CPU time reported in Table III for the 880-node system by [27] is obtained using a relaxed model of the reconfiguration problem (quadratic programming). There are no simulation results for this system using a more accurate model proposed in [27], which is based on mixed-integer conic programming. Nevertheless, it is expected to take longer than the time reported in Table III for the more accurate method of [27] to converge. In [40], the problem is formulated as a mixed-integer nonlinear programming problem and is solved using the B&B algorithm.

Although the time elapsed to solve the MIQP problem may be relatively long, one should note that this happens because the program is forced to provide the *proven optimal solution* (zero optimality gap). In many cases, the program reaches the real optimal solution quickly, but it takes a long time to prove that this is the optimal solution. For instance, for the 119-node system, the reported optimal solution is reached in about 16 s, but it takes another 23 s for the algorithm to prove its optimality. As a result, there are two ways to reduce the solution time substantially:

1) by defining a limit for the solution time;
2) by choosing a greater relative optimality gap, for example, 5%.

The CPU times considering a 5% relative optimality gap for the 14, 33, 70, 84, 119, 136, and 880-node systems are 0.12, 2.1, 2.9, 3.6, 13.5, 52.5, and 596 s, respectively. In many cases, the results obtained within the gap of 5% are actually within the gap of 1%. However, it takes longer for the solver to prove this. For example, the optimal solutions for the 14 and 33-node systems are the same even if a 5% gap is assumed.

The optimal reconfiguration for loss reduction improves the voltage profile and minimizes the reactive power losses at the same time. This can be confirmed by checking the minimum and average values for the nodal voltages and the reactive power losses reported in Table III.

As mentioned before, the effect of the loads' voltage dependency on the network power losses are inevitable. In order to show these effects, the 70-node test system is chosen and the optimal configuration is maintained. Fig. 3(a) illustrates the impact of C_Z on active and reactive power losses. The total power consumption of the loads is shown in Fig. 3(b). As reported in Fig. 3(a) and (b), the active and reactive power losses and the total consumption of the loads are relatively sensitive to C_Z,

TABLE IV
OPTIMAL CONFIGURATIONS FOR TEST SYSTEMS

System	Open Lines
14-node	6-8,7-9,5-14
33-node	7-8,9-10,14-15,32-33,25-29
70-node	14-15,9-38,15-67,49-50,39-59,38-43,9-15,21-27,28-29, 62-65,40-44
84-node	7-6,13-12,18-14,26-16,32-28,34-33,39-38,43-11,72-71, 83-82,55-5,41-42,63-62
119-node	23-24,26-27,35-36,41-42,44-45,51-65,53-54,61-62,74-75,77-78,86-113,95-100,101-102,89-110,114-115
136-node	6-7,10-32,57-61,78-125,20-130,137-138,59-145,139-154,141-154,155-156,154-204,211-212,138-217,125-219,141-220,222-223,144-145,43-46,63-64,130-131, 214-215
880-node	89-90,136-137,146-147,164-165,195-196,287-288,293-294,290-312,318-336,414-415,417-418,457-458,499-500,601-602,621-622,634-635,636-637,642-643,653-704,736-824,848-849,345-500,463-824,460-440,580-800, 850-250,10-470

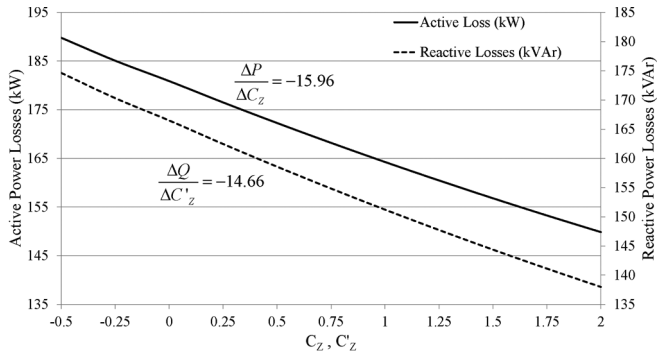

Fig. 3. Optimal configuration analysis for different types of load voltage dependencies in the 70-node test system ($C_Z = C'_Z$). (a) Active and reactive power losses. (b) Total active and reactive power consumptions.

which indicates their voltage dependency. This, in fact, emphasizes the importance of the load voltage dependency modeling in power system analysis. Real data for the values of the parameters C_Z and C'_Z will be accessible upon deployment of the advanced metering infrastructure (AMI) in distribution systems.

1) Limiting the Number of Switching Actions: In Section IV-A, no limit on the number of switching actions S was assumed. In this part, it is shown that slightly different values for losses can be achieved with a smaller S. Limiting S may also reduce the solution time for the B&B algorithm. Table V shows the active losses achieved for the corresponding limit on S in the optimal configuration. As can be seen, usually the first few switching actions produce the largest reduction in the total losses. For example, by halving the limit on S, only about an 0.9% increase in the losses was observed for the 136-node system. The CPU time was also reduced compared to the previous case, while the number of integer variables is essentially the same. It should be noted that the solution speed for a mixed-integer problem is mainly governed by the number of integer variables. In a real system, the number of switches is small as compared to the number of branches; hence, the computation time may not be a challenge for the application of the proposed framework for large-scale systems.

In general, especially with mechanical switches, it is desired to have the best configuration with the minimum number of required switching actions. In order to compromise between these two objectives, a multiobjective optimization problem may be defined which minimizes both the losses and the number of switching actions simultaneously. This requires an estimation of the monetary cost of each switching operation and of the losses. Since these data are not available to the authors, in the examples an arbitrary limit on the number of switching actions is used.

TABLE V
RESULTS OBTAINED BY ASSUMING A LIMIT ON THE NUMBER OF SWITCHING ACTIONS *

14-node	S^{max}	4	2	0	
	P_{loss} (kW)	553.7	570.7	593.9	
33-node	S^{max}	8	4	0	
	P_{loss} (kW)	122.8	126.3	167.3	
70-node	S^{max}	10	6	0	
	P_{loss} (kW)	172.3	173.9	189.2	
84-node	S^{max}	16	8	4	0
	P_{loss} (kW)	424.2	426.5	437.7	470.2
119-node	S^{max}	24	10	4	0
	P_{loss} (kW)	765.9	798.1	853.8	1029.8
136-node	S^{max}	24	12	4	0
	P_{loss} (kW)	258.2	260.8	263.4	287.4
880-node	S^{max}	48	12	4	0
	P_{loss} (kW)	958.7	1098.3	1470.0	2858.8

* The results are obtained assuming: $C_Z = C'_Z = 0.5$.

As part of system planning, it is sometimes needed to find the best place to install a switch between two feeders. The proposed framework is capable of doing this task in a similar way as the optimal network reconfiguration.

B. Optimal ULTC Adjustment

In this part, it is assumed that the substation transformers are equipped with ULTC capability. These transformers may have an algorithm to maintain the voltage at a certain level which is usually based on *local* measurements. However, by looking at the whole network and trying to find the optimum tap position for all the voltage regulators at the same time, globally optimum tap settings can be achieved. The model proposed in Section III-C for ULTC is used. Twenty steps of 0.5% are assumed for each voltage regulator. The 70-node test system is selected for the simulations due to its poor voltage profile. There are four feeders in this system. Without loss of generality, it is assumed that each feeder is fed by a separate ULTC transformer, which is located at the first section of that feeder. In a more general case, the voltage regulators may exist anywhere else in the network.

In the first case, the initial configuration of the network is maintained. Table VI shows the results for the optimum tap positions when only ULTC adjustments are performed. Loads are modeled by $C_Z = C'_Z = 0.5$. About 14.4% reduction in losses was achieved by optimally adjusting the ULTCs. In the second case, the optimal reconfiguration and ULTC adjustments are done simultaneously. The results are also shown in Table VI. In this case, 28.7% reduction in losses was achieved. Note that the minimum voltage limit is assumed to be 0.92 p.u. for this scenario.

C. Optimal Control of Capacitor Banks

Since there are no capacitor banks in the original version of the 70-node system, the proposed algorithm is employed to recommend the best places to install new capacitors. The total

TABLE VI
ULTC ADJUSTMENT AND OPTIMAL RECONFIGURATION FOR THE 70-NODE SYSTEM

Control Action	P_{loss} (kW)	V_{avg} (P.U.)	Voltage Regulator Ratio			
			1-2	1-16	1-30	1-51
ULTC	156.7	0.964	1.015	1.015	1.005	1.005
ULTC+Reconf.	130.5	0.968	1.0175	1.015	1.005	1.005

TABLE VII
OPTIMAL CAPACITOR CONTROL, RECONFIGURATION AND ULTC ADJUSTMENT FOR THE 70-NODE SYSTEM

Control Action	P_{loss} (kW)	V_{avg} (P.U.)	Voltage Regulator Ratio			
			1-2	1-16	1-30	1-51
Cap.	141	0.968	1.000	1.000	1.000	1.000
Cap. + ULTC	122.4	0.975	1.010	1.010	1.005	1.005
Cap. + Reconf.	131.9	0.970	1.000	1.000	1.000	1.000
Cap. + Reconf. + ULTC	112.6	0.977	1.010	1.015	1.005	1.005

installed capacity is limited to 2.4 MVAR, with steps of 400 kVAR. The results of this study are shown in Table VII. First, only capacitor placement is studied. The solution indicates that 400 kVAR should be installed at nodes 4, 28, 39, 47, 58, and 66. The capacitor placement results in a 25.4% reduction in the losses. In the second study, capacitor placement and ULTC adjustments are done simultaneously. This study shows that 400 kVAR of capacitors should be installed at nodes 5, 26, 39, 49, 59, and 62, which shows fairly close location results with respect to the previous case. About a 35.3% reduction in losses was achieved in this case. In the third study, capacitor control and reconfiguration are done simultaneously. The new locations for the capacitors are nodes 4, 21, 42, 47, 59, and 62. About a 30.3% reduction in losses was achieved.

In a fourth case, capacitor control, ULTC adjustment, and reconfiguration are done simultaneously and the results are shown in the last row of Table VII. About a 40.5% loss reduction is achieved by utilizing all the controllers. The locations of capacitors in this case are nodes 27, 41, 47, 62, and 68. The open switches in this case are 9–15, 14–15, 15–67, 26–27, 37–38, 39–59, 42–43, 44–45, 49–50, 63–64, and 65–66.

Based on the simulations, by optimally controlling the ULTCs and installing capacitors in appropriate locations, the system performance will increase significantly. The losses are highly dependent on the voltage profile of the network. This fact can also be mathematically interpreted from (8). The effect of reconfiguration will be less dramatic when extensive voltage controlling devices are already present in the system. However, extensive deployment of voltage controlling devices is expensive. In addition, the benefits of reconfiguration are not limited to loss reduction and voltage profile improvement but also extend to load balancing among feeders and increasing system reliability. Also, in many cases, it is not possible to have ULTCs on every feeder. For instance, there are transformers that may feed more than 20 outgoing feeders. In such instances, reconfiguration plays an influential role in optimizing the system performance.

V. CONCLUSION

Distribution system performance has been optimized by introducing a robust framework which optimally controls the network configuration, voltage regulators and switchable capacitor banks. Besides the simplicity of the formulation, available software for solving MIQP problems provide many options for the user to tune the solver for the best performance on a specific problem. Moreover, the significance of load modeling in distribution system analysis has been shown. The number of switching actions, which may be a concern for system operators, can be limited to a point at which it does not influence the optimum solution meaningfully and accelerates the solution process. The optimized adjustment of voltage regulators has been shown to have a substantial impact on system performance in terms of losses and voltage profile. The increased interest toward advanced metering infrastructure and the flexibilities provided by these equipments enable the system operator to have a good estimation of the loads' voltage dependency which is needed for the linear power-flow algorithm.

REFERENCES

[1] K.-H. Kim and S.-K. You, "Voltage profile improvement by capacitor placement and control in unbalanced distribution systems using GA," in *Proc. IEEE Power Eng. Soc. Summer Meeting*, 1999, vol. 2, pp. 800–805.
[2] M. E. Baran and F. F. Wu, "Network reconfiguration in distribution systems for loss reduction and load balancing," *IEEE Trans. Power Del.*, vol. 4, no. 2, pp. 1401–1407, Apr. 1989.
[3] Q. Zhou, D. Shirmohammadi, and W. H. E. Liu, "Distribution feeder reconfiguration for service restoration and load balancing," *IEEE Trans. Power Syst.*, vol. 12, no. 2, pp. 724–729, May 1997.
[4] B. Amanulla, S. Chakrabarti, and S. N. Singh, "Reconfiguration of power distribution systems considering reliability and power loss," *IEEE Trans. Power Del.*, vol. 27, no. 2, pp. 918–926, Apr. 2012.
[5] A. A. Sallam and O. P. Malik, *Electric Distribution Systems*. Hoboken, NJ, USA: Wiley, 2011.
[6] S. Civanlar, J. J. Grainger, H. Yin, and S. S. H. Lee, "Distribution feeder reconfiguration for loss reduction," *IEEE Trans. Power Del.*, vol. 3, no. 3, pp. 1217–1223, Jul. 1988.
[7] C. Ababei and R. Kavasseri, "Efficient network reconfiguration using minimum cost maximum flow-based branch exchanges and random walks-based loss estimations," *IEEE Trans. Power Syst.*, vol. 26, no. 1, pp. 30–37, Feb. 2011.
[8] V. Farahani, B. Vahidi, and H. A. Abyaneh, "Reconfiguration and capacitor placement simultaneously for energy loss reduction based on an improved reconfiguration method," *IEEE Trans. Power Syst.*, vol. 27, no. 2, pp. 587–595, May 2012.
[9] G. Raju and P. R. Bijwe, "An efficient algorithm for minimum loss reconfiguration of distribution system based on sensitivity and heuristics," *IEEE Trans. Power Syst.*, vol. 23, no. 3, pp. 1280–1287, Aug. 2008.
[10] J. Mendoza, R. Lopez, D. Morales, E. Lopez, P. Dessante, and R. Moraga, "Minimal loss reconfiguration using Genetic Algorithms with restricted population and addressed operators: Real application," *IEEE Trans. Power Syst.*, vol. 21, no. 2, pp. 948–954, May 2006.
[11] E. R. Ramos, A. G. Exposito, J. R. Santos, and F. L. Iborra, "Path-based distribution network modeling: Application to reconfiguration for loss reduction," *IEEE Trans. Power Syst.*, vol. 20, no. 2, pp. 556–564, May 2005.
[12] E. M. Carreno, R. Romero, and A. Padilha-Feltrin, "An efficient codification to solve distribution network reconfiguration for loss reduction problem," *IEEE Trans. Power Syst.*, vol. 23, no. 4, pp. 1542–1551, Nov. 2008.
[13] B. Enacheanu, B. Raison, R. Caire, O. Devaux, W. Bienia, and N. HadjSaid, "Radial network reconfiguration using Genetic Algorithm based on the Matroid theory," *IEEE Trans. Power Syst.*, vol. 23, no. 1, pp. 186–195, Feb. 2008.

[14] H. D. de Macedo Braz and B. A. de Souza, "Distribution network reconfiguration using Genetic Algorithms with sequential encoding: Subtractive and additive approaches," *IEEE Trans. Power Syst.*, vol. 26, no. 2, pp. 582–593, May 2011.
[15] Y.-J. Jeon, J.-C. Kim, J.-O. Kim, J.-R. Shin, and K. Y. Lee, "An efficient Simulated Annealing Algorithm for network reconfiguration in large-scale distribution systems," *IEEE Trans. Power Del.*, vol. 17, no. 4, pp. 1070–1078, Oct. 2002.
[16] A. Y. Abdelaziz, R. A. Osama, and S. M. El-Khodary, "Reconfiguration of distribution systems for loss reduction using the Hyper-Cube Ant Colony optimisation algorithm," *IET Gen. Transm. Distrib.*, vol. 6, no. 2, pp. 176–187, Feb. 2012.
[17] C. Chang, "Reconfiguration and capacitor placement for loss reduction of distribution systems by Ant Colony search algorithm," *IEEE Trans. Power Syst.*, vol. 23, no. 4, pp. 1747–1755, Nov. 2008.
[18] R. Srinivasa Rao, S. V. L. Narasimham, M. R. Raju, and A. S. Rao, "Optimal network reconfiguration of large-scale distribution system using Harmony Search Algorithm," *IEEE Trans. Power Syst.*, vol. 26, no. 3, pp. 1080–1088, Aug. 2011.
[19] C. Su and C. Lee, "Network reconfiguration of distribution systems using improved mixed-integer hybrid differential evolution," *IEEE Trans. Power Del.*, vol. 18, no. 3, pp. 1022–1027, Jul. 2003.
[20] A. Mendes, N. Boland, P. Guiney, and C. Riveros, "Switch and tap-changer reconfiguration of distribution networks using Evolutionary Algorithms," *IEEE Trans. Power Syst.*, vol. 28, no. 1, pp. 85–92, Feb. 2013.
[21] A. C. Santos, A. C. B. Delbem, J. B. A. London, and N. G. Bretas, "Node-Depth encoding and multiobjective evolutionary algorithm applied to large-scale distribution system reconfiguration," *IEEE Trans. Power Syst.*, vol. 25, no. 3, pp. 1254–1265, Aug. 2010.
[22] M. Tsai and F. Hsu, "Application of grey correlation analysis in evolutionary programming for distribution system feeder reconfiguration," *IEEE Trans. Power Syst.*, vol. 25, no. 2, pp. 1126–1133, May 2010.
[23] H. Salazar, R. Gallego, and R. Romero, "Artificial Neural Networks and clustering techniques applied in the reconfiguration of distribution systems," *IEEE Trans. Power Del.*, vol. 21, no. 3, pp. 1735–1742, Jul. 2006.
[24] W. Wu and M. Tsai, "Application of enhanced integer coded Particle Swarm Optimization for distribution system feeder reconfiguration," *IEEE Trans. Power Syst.*, vol. 26, no. 3, pp. 1591–1599, Aug. 2011.
[25] H. M. Khodr, J. Martinez-Crespo, M. A. Matos, and J. Pereira, "Distribution systems reconfiguration based on OPF using Benders decomposition," *IEEE Trans. Power Del.*, vol. 24, no. 4, pp. 2166–2176, Oct. 2009.
[26] R. A. Jabr, R. Singh, and B. C. Pal, "Minimum loss network reconfiguration using mixed-integer convex programming," *IEEE Trans. Power Syst.*, vol. 27, no. 2, pp. 1106–1115, May 2012.
[27] J. A. Taylor and F. S. Hover, "Convex models of distribution system reconfiguration," *IEEE Trans. Power Syst.*, vol. 27, no. 3, pp. 1407–1413, Aug. 2012.
[28] J. R. Marti, H. Ahmadi, and L. Bashualdo, "Linear power flow formulation based on a voltage-dependent load model," *IEEE Trans. Power Del.*, vol. 28, no. 3, pp. 1682–1690, Jul. 2013.
[29] IBM – Mathematical Programming: Linear Programming, Mixed-Integer Programming and Quadratic Programming – IBM ILOG CPLEX Optimizer – Software. [Online]. Available: http://www-01.ibm.com/software/integration/optimization/cplex-optimizer/
[30] Gurobi Optimizer 5.0 – State-of-the-Art Mathematical Programming Solver. [Online]. Available: http://www.gurobi.com/
[31] L. M. Hajagos and B. Danai, "Laboratory measurements and models of modern loads and their effect on voltage stability studies," *IEEE Trans. Power Syst.*, vol. 13, no. 2, pp. 584–592, May 1998.
[32] E. M. L. Beale and J. A. Tomlin, "Special facilities in a general mathematical programming system for non-convex problems using ordered sets of variables," presented at the 5th Int. Conf. Oper. Res., London, U.K., 1969.
[33] F. Glover, "Improved linear integer programming formulations of nonlinear integer problems," *Manage. Sci.*, vol. 22, no. 4, pp. 455–460, Dec. 1975.
[34] J. C. Das, *Power System Analysis: Short-Circuit Load Flow and Harmonics*. Boca Raton, FL, USA: CRC, 2002.
[35] D. Das, "A fuzzy multiobjective approach for network reconfiguration of distribution systems," *IEEE Trans. Power Del.*, vol. 21, no. 1, pp. 202–209, Jan. 2006.
[36] D. Zhang, Z. Fu, and L. Zhang, "An improved TS algorithm for loss-minimum reconfiguration in large-scale distribution systems," *Elect. Power Syst. Res.*, vol. 77, no. 5-6, pp. 685–694, 2007.
[37] J. R. S. Mantovani, F. Casari, and R. A. Romero, "Reconfiguração de sistemas de distribuição radiais utilizando o critério de queda de tensão," *SBA Controle Automação*, vol. 11, no. 3, pp. 150–15, Nov. 2000.
[38] R. Kavasseri and C. Ababei, REDS: Repository of Distribution Systems, North Dakota State Univ., Fargo, ND, USA, 2013. [Online]. Available: http://venus.ece.ndsu.nodak.edu/~kavasseri/reds.html
[39] *"AIMMS Language Reference,"* Paragon Decision Technology, Bellevue, WA, USA.
[40] M. Lavorato, J. F. Franco, M. J. Rider, and R. Romero, "Imposing radiality constraints in distribution system optimization problems," *IEEE Trans. Power Syst.*, vol. 27, no. 1, pp. 172–180, Feb. 2012.

Hamed Ahmadi (S'12) received the B.Sc. and M.Sc. degrees in electrical engineering from the University of Tehran, Tehran, Iran, in 2009 and 2011, respectively, and is currently pursuing the Ph.D. degree in electrical engineering at the University of British Columbia, Vancouver, BC, Canada.

His research interests include distribution system analysis, power system stability and control, smart grids, and high-voltage engineering.

José R. Martí (M'80–SM'01–F'02) received the M.Eng. degree in electric power (M.E.E.P.E.) from Rensselaer Polytechnic Institute, Troy, NY, USA, in 1974, and the Ph.D. degree in electrical engineering from the University of British Columbia, Vancouver, BC, Canada, in 1981.

He is known for his contributions to the modeling of fast transients in large power networks, including component models and solution techniques. Particular emphasis in recent years has been on the development of distributed computational solutions for real-time simulation of large systems and integrated multisystem solutions. He is a Professor of electrical and computer engineering at the University of British Columbia and a Registered Professional Engineer in the Province of British Columbia, Canada.